Resolving antiferromagnetic states in magnetically coupled amorphous Co-Si-Si multilayers by soft x-ray resonant magnetic scattering

S. M. Valvidares,[1,*] C. Quirós,[2] A. Mirone,[1] J.-M. Tonnerre,[3] S. Stanescu,[1,†] P. Bencok,[1,‡] Y. Souche,[3] L. Zárate,[2] J. I. Martín,[2] M. Vélez,[2] N. B. Brookes,[1] and J. M. Alameda[2]

[1]*European Synchrotron Radiation Facility, Boîte Postale 220, 38043 Grenoble Cedex, France*

[2]*Departamento de Física, Universidad de Oviedo–CINN, Calle Calvo Sotelo s/n, 33007 Oviedo, Spain*

[3]*Institut Néel, CNRS and Université Joseph Fourier, Boîte Postale 166, F-38042 Grenoble Cedex 9, France*

(Received 3 March 2008; revised manuscript received 21 May 2008; published 8 August 2008)

Soft x-ray resonant magnetic scattering (SXRMS) has been used to probe the interlayer coupling in amorphous ferromagnetic/semiconductor multilayers. It is shown that the $[Co_{73}Si_{27}$ (50 Å)/Si (30 Å)] system exhibits an antiferromagnetic (AF) coupling at low fields. Moreover, another aspect of SXRMS effect is reported. Using circularly polarized photons, a shift in the AF order Bragg peaks' position is observed and related to two opposite AF states with the spin direction longitudinally aligned. As a consequence, the sensitivity of SXRMS to AF domains having the same spin axis but opposite senses is shown. A physical explanation for the origin of this effect is provided in terms of magnetic-resonant-refraction corrections to Bragg's angle, taking into account the phase shifts between layers with opposite magnetization directions at different in-depth positions. Numerical simulations are performed that reproduced the experimental observations.

DOI: 10.1103/PhysRevB.78.064406 PACS number(s): 75.50.Ee, 78.70.Ck, 78.67.Pt

I. INTRODUCTION

A detailed characterization of magnetic configuration in multilayered magnetic systems is challenging since depth resolved magnetic techniques are required,[1–3] and standard methods are usually sensitive only to net magnetization. A powerful solution to investigate antiferromagnetic (AF) ordering can be found by using scattering techniques such as soft x-ray resonant magnetic scattering (SXRMS) (Ref. 4) or neutron diffraction.[1,2] The case of SXRMS is especially interesting since it combines the depth sensitivity inherent to scattering phenomena with the chemical and electronic-shell selectivity given by the resonant condition. It also has the advantage of offering a broad accessible q range, allowing one to probe several AF half-order Bragg peaks.[5] As a consequence, the technique has been increasingly used in recent years to characterize the magnetism of AF exchange-coupled multilayers.[6] However, it is worth mentioning that, although the basic principles of SXRMS are already well established, the technique is in continuous development and is being used to address problems of increasing complexity related to interface magnetism, domain correlations, coherent diffraction, time resolved phenomena, determination of x-ray resonant optical constants, or magnetic correlation spectroscopy.[5–16]

In this work, SXRMS is used with an unusual polarization/magnetization configuration for the investigation of an interlayer-coupled system. Usually, the applied magnetic field is oriented longitudinally (in the film plane and in the diffraction plane) and circular or linear polarization may be employed. When the amplitude of the magnetic field is reduced, the two orientations of the spin axis "move away" to stabilize transversally to the diffraction plane. Here, as it will be discussed later, a uniaxial anisotropy imposes the AF state to remain longitudinally aligned. The use of circularly polarized light reveals a change in the position of magnetic half-order peaks related to two opposite AF states (or opposite photon helicities), opening the possibility to determine the AF domain orientation. In addition, the results also show that for the studied multilayers, the remanent state obtained with zero net magnetization is not formed by an equally populated distribution of opposite AF domains but by a distribution with a predominant orientation of the AF domains that reverses depending on the branch of the hysteresis loop that is being probed.

The system where these effects have been observed belongs to the poorly understood case of magnetic layers separated by semiconducting spacers.[17–21] It consists of a multilayer built up with layers of an amorphous Co-Si magnetic alloy separated by Si nonmagnetic spacers. Multilayers based on a semiconductor spacer, such as Si, combined with an amorphous magnetic film, may benefit from the large flexibility in control and design of, almost at wish, magnetic properties such as anisotropy, coercive field, magnetic moments, and critical temperatures. These multilayers can be fabricated by low cost techniques such as sputtering. This Co-Si system has been recently shown to couple antiferromagnetically with switching fields in the order of few oersteds.[22,23] Interestingly, a much stronger AF coupling has been also recently reported in polycrystalline Co/Si multilayers.[24] However, up to now, the evidence of the AF coupling has been based on accepted but indirect measurements such as hysteresis loops.[22–24]

In the following, SXRMS is used to confirm the presence of the AF alignment and investigate the AF configuration. The angle dependent reflectivity curves are first analyzed. Then, hysteresis loops at a fixed energy and at fixed angles, chosen close to the AF Bragg peak and chemical Bragg peak, are discussed. The domain orientation dependent shift of half-order peaks is shown. An insight into the physical origin of this effect is then given by additional measurements on a two period multilayer and by analytical discussion of the case of this simpler stacking. Finally, numerical simulations are used to model the reflectivity signal for the more complex case of a ten period multilayer.

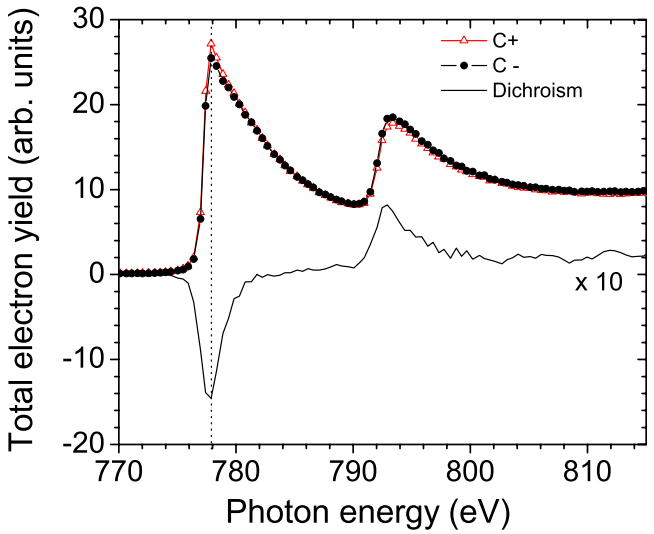

FIG. 1. (Color online) Photon energy dependence of the Co $L_{\text{II-III}}$ absorption edge for C_+ and C_- polarizations measured in total electron yield (TEY) under a saturating longitudinal applied magnetic field. The SXRMS measurements were carried out in the vicinity of the maximum of the Co L_{III} edge, 778 eV, indicated by the dotted line. The corresponding dichroic signal ($\times 10$) is also shown as a continuous line.

II. RESULTS AND DISCUSSION

For this study, different samples have been grown by dc-magnetron cosputtering on top of Si(111) substrates.[22] The nominal structure is $[\text{Si}\ (30\ \text{Å})/\text{Co}_{73}\text{Si}_{27}\ (50\ \text{Å})]_{n=2,10}/30\ \text{Å}\ \text{Si}/\text{substrate}$. SXRMS measurements were carried out using an under vacuum four-circle diffractometer at ESRF BL-ID08. Magnetic fields of up to 30 Oe, with 0.05 Oe resolution, were applied always longitudinally, that is, in the photon-scattering plane and in the sample surface plane. The sample has been rotated around the azimuth and oriented so that the magnetic field is parallel to the direction of the magnetic easy axis (within $\sim 10°$ of misalignment). The photon polarization was controlled from $\sim 100\%$ circular right (C_+) or left (C_-) to $\sim 100\%$ linear σ or linear π, and the photon energy has been tuned in the vicinity of the Co L_{III} edge (778 eV). Figure 1 displays the Co $L_{\text{II-III}}$ absorption spectrum for the two opposite circular polarization states as measured by total electron yield as well as the corresponding dichroic signal.

The shape of the curve reminds one of that of a pure Co L edge but with broader peaks, most likely due to the fact that this sample is a cobalt silicide, not a pure Co one. Also, the amplitude of the dichroic signal is much smaller than that of pure Co due to the difference in the saturation magnetization, which is about 1 order of magnitude smaller for this amorphous cobalt silicide.

The samples have been characterized by transverse magneto-optical Kerr effect (TMOKE). The hysteresis loop of the ten period sample is displayed in the inset of Fig. 2, where the vertical scale corresponds to the standard normalization of Kerr measurements: $\delta=(I^{\text{field}}-I_0)/I_0$, where I^{field} is the intensity at a given magnetic field and I_0 is the intensity

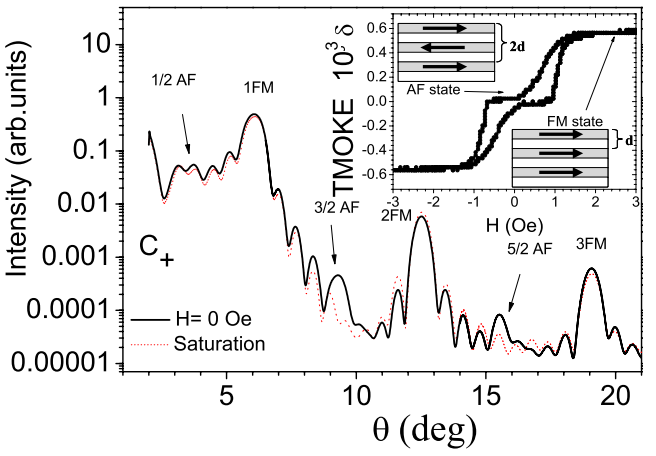

FIG. 2. (Color online) SXRMS vs θ for saturation, $H=10$ Oe (red thin line), and remanence, $H=0$ Oe after negative saturation (black thick line), in a $[\text{Si}\ (30\ \text{Å})/\text{Co}_{73}\text{Si}_{27}\ (50\ \text{Å})]_{10}$ multilayer using circularly polarized light at 778 eV. The inset shows a reference TMOKE easy axis loop, measured with compensation for the earth´s magnetic field, showing the multilayer AF-state plateau.

at remanence. The Kerr loops suggest that the samples have two main characteristics: (i) AF coupling with low switching fields, ~ 1 Oe, as it can be deduced from the plateau at remanence (inset of Fig. 2), and (ii) uniaxial in-plane magnetic anisotropy, on the order of 20 Oe, defined by the oblique incidence during growth.[22] It is worth noting that the observation of such a weak AF coupling is possible due to the soft magnetic behavior, $H_C \sim 0.6$ Oe, of single thin layers of this amorphous $\text{Co}_{73}\text{Si}_{27}$ alloy. Moreover, in this case, the energy balance between the weak AF coupling and the uniaxial anisotropy prevents magnetization rotations away from the easy axis during the reversal process, so that the magnetization remains parallel to the easy axis at the AF state and during the whole hysteresis loop, reversing through domain-wall motion[22] and not by rotations through transverse states.

In order to investigate this scenario, specular SXRMS has been used to probe the magnetic periodicities normal to the sample surface. Figure 2 shows the reflectivity curves as a function of the incidence angle θ for an $n=10$ multilayer. The reflectivity has been measured at about 777 eV without any applied field and at saturation ($H=10$ Oe). The reflectivity curve for the saturated state (thin line) exhibits three intense peaks related to the first three orders of the structural periodicity of the multilayer, corresponding to a period of 74 Å, in good agreement with the 80 Å nominal value. Between the multilayer Bragg peaks, labeled as FM (ferromagnetic), well-defined Kiessig interference fringes, corresponding to a total thickness of 739 Å, are observed. This shows that the soft x rays probe the whole multilayer thickness even at the maximum of absorption. The most relevant feature of Fig. 2 are the extra peaks observed in the remanent state at zero field (thick line), which correspond to half-integer order positions, and are, by comparison to the reflectivity in the saturated state, the unequivocal fingerprint of magnetic AF ordering of the neighboring $\text{Co}_{73}\text{Si}_{27}$ layers. Interestingly, the widths at half maximum of both Bragg and AF peaks are equal so they relate to a similar probed thickness, which

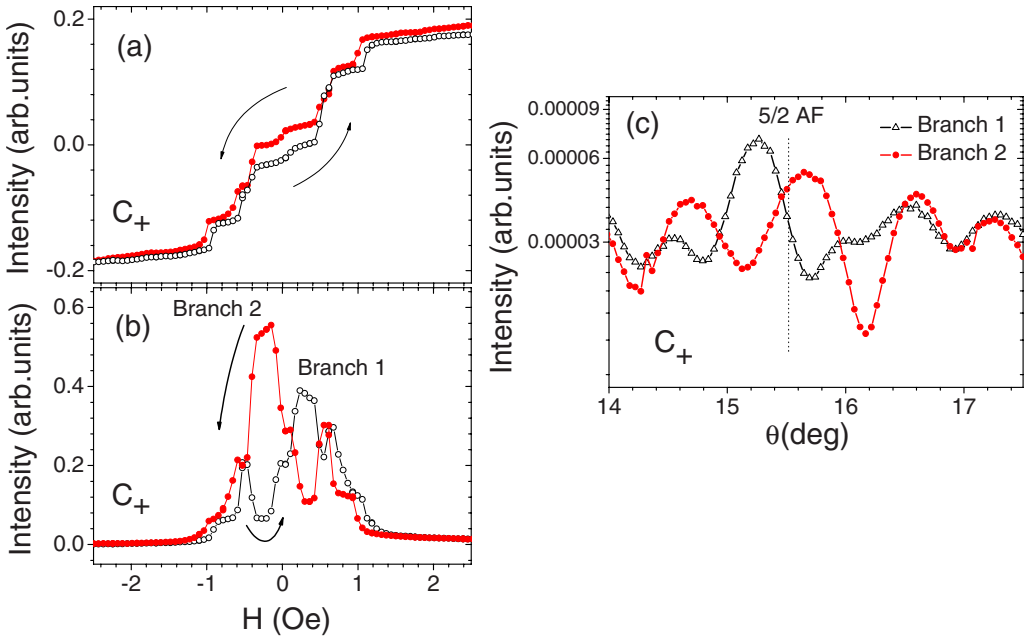

FIG. 3. (Color online) X-ray hysteresis loops of the $n=10$ multilayer using C_+ light (arrows indicate the sense of the loop; loop branches in red and black): (a) at third FM peak ($\theta=19.0°$); (b) at 5/2 AF peak ($\theta=15.7°$). (c) Reflectivity SXRMS curves around the 5/2 AF peak acquired with C_+ polarization for $n=10$ multilayer at two magnetic states: remanence AF state of branch 1 (empty circles) and remanence AF state of branch 2 (filled circles). The dotted vertical line shows the nominal 5/2 AF-peak position.

leads to the important conclusion that the AF state is vertically correlated through the complete thickness of the multilayer.

An insight into the building up and breaking of the multilayer AF state, as well as into the whole magnetization process, can be gained by comparing x-ray magnetic hysteresis loops recorded at a FM Bragg peak and at an AF Bragg peak.[5,7] Figures 3(a) and 3(b) show the measurements, in the longitudinal geometry applied, at the third FM peak and at the 5/2 AF peak, respectively, where the intensity has been normalized in the same way as the TMOKE loop in the inset of Fig. 2. (For the case of the AF loop, the reference intensity I_0 is the saturation intensity, instead of the remanent one.) The Bragg-peak loop reproduces the basic feature of the TMOKE measurement with visible light: a plateau in the proximity of zero field related to the stabilization of the compensated AF state. However, this FM loop, as well as the AF-peak loop, exhibits some extra jumps. It is worth mentioning that the extra jumps observed in the SXRMS loops compared to those in TMOKE loops reflect the different natures of the scattering phenomena used by both techniques. Specular SXRMS is more sensitive to interference processes that may appear in incomplete AF domain configurations and that for the case of TMOKE, will be averaged, leading to a smoother behavior of the loop. The extra jumps in the FM loop [Fig. 3(a)] indicate that the reversal process develops through intermediate stable states corresponding to different AF configurations. This interpretation is also substantiated by the abrupt changes in the intensity of the half-order Bragg peak [Fig. 3(b)] mostly occurring when a jump is observed in the loop measured on the FM Bragg peak. Indeed, the AF-peak loop can be interpreted in a similar way as the FM-peak loop: when the magnetic field is strong enough to fully align the ferromagnetic $Co_{73}Si_{27}$ layers, the intensity of the AF peak is zero; when the magnetic field is reduced, the AF coupling starts to be dominant and some magnetic layers reverse up to yield an AF contribution in the multilayers stacking, leading to the onset of the AF-peak intensity. Besides, this explicitly shows that the multilayer AF state is destroyed by the application of weak magnetic fields above ~1 Oe, in perfect agreement with the TMOKE plateau width (inset of Fig. 2). The different AF configurations obtained as the applied magnetic field is reduced may consist of an increasing number of layers antiferromagnetically aligned and cover an increasing fraction of the sample surface to reach a fully compensated antiferromagnetic stacking, which in turn corresponds to a maximum in the intensity of the half-order Bragg loop. Such a general behavior (without the jumps) has already been observed and discussed by comparing the AF-peak loop with the dependence of the giant magnetoresistance ratio on the applied magnetic field.[5,7]

In spite of this general interpretation of Fig. 3 loops, the depressed part just before the maximum in Fig. 3(b), where a stronger intensity is expected, associated with the symmetric behavior of the two branches, suggests that more subtle and sophisticated effects may play a significant role close to the remanent state. Some of these effects can be revealed when measuring, at the same energy and using the same polarization state, the reflectivity curves around the 5/2 AF reflectivity peak for two different magnetic states [see Fig. 3(c)]: the AF remanent magnetic state when coming from negative magnetic field values [branch 1 of loop in Fig. 3(b)] and the AF remanent state when the magnetic field is decreased (branch 2). The result shows an unexpected behavior that is a shift of ~0.5° in the AF-peak position depending on the way the compensated AF magnetic state is established. It is well

known that beyond the energy dependence of the angular position from the Bragg law, a resonant shift in the FM Bragg-peak position can be observed when the reflectivity is measured in the vicinity of the L edges[4,5,7,11] as well as a shift in the AF-peak position.[7] Here the incident-photon energy is the same and is not at the origin of the shift. It is also well known that at the same energy close to resonance, reversing the magnetization or reversing the helicity of the incoming photons may lead to a shift in the FM Bragg-peak position.[4,5,7,11] However, here, the same polarization state has been used and we are measuring the reflectivity from the AF peak at remanence, where no net magnetization is observed. Besides, such an AF-peak shift, in the investigation by SXRMS dedicated to antiferromagnetic coupling in metallic multilayers, has never been reported.[4,5,7,11] It has to be pointed out that, at contrary to our system, the direction of the magnetization in the AF state for the previously investigated systems tends to be perpendicular to the nonsaturating applied magnetic field. The results shown in Fig. 3(c) suggest that the shift in the AF Bragg-peak position could be related to a difference in the AF configuration. Depending on the magnetic history (branch 1 or 2), the AF configuration at remanence may exhibit an opposite structure along the growth axis. Therefore, the building up of the AF ordering does not lead only to the growth and narrowing of the corresponding half-order peaks, as it has been reported in other multilayer systems,[4,5,7] but also, under certain circumstances, to a change in their positions. In fact, the oscillations observed in the AF loop in Fig. 3(b), when the AF state is being formed for both branches, may be related to rearrangements of the magnetization orientation of the layers leading to intensity changes caused by the AF-peak shift.

No previous observation of an AF Bragg-peak shift has been reported. This is in line with the idea that, in a first approximation, a shift in the AF-peak position would not be *a priori* expected, since SXRMS is, to first order, linear in the magnetization and there is no net magnetization in the AF state. Nevertheless, if a nonkinematical approach is used for the Bragg law, so that refraction and absorption effects are considered in the propagation of x rays across a multilayer,[25] shifts in the reciprocal space position of the multilayer peak may appear.[11,26] In the case of SXRMS, refraction and absorption will depend on the magnetic state of the magnetic layers, which can affect the reciprocal space position of FM or AF peaks. The mechanism for this effect can be qualitatively illustrated by introducing *ad hoc* the magnetic resonant corrections to the optical index[27] in the formula for (nonmagnetic) anomalous diffraction corrections due to resonant refraction and absorption effects of the Bragg angle θ_B, given by a shift $\Delta\theta$ (Ref. 26):

$$\theta_B + \Delta\theta = \theta_B + \frac{\bar{\delta}}{\sin\theta_B \cos\theta_B} - \frac{\Delta\beta\Delta\delta}{\bar{\beta}\sin\theta_B\cos\theta_B}\left[\frac{\sin(m\pi/2)}{m\pi}\right]^2, \quad (1)$$

where an antiferromagnetically coupled multilayer composed of alternating magnetic layers of equal thickness and opposite magnetizations has been considered, $\bar{\delta}$ and $\bar{\beta}$ are average values over a multilayer period, and $\Delta\delta$ and $\Delta\beta$ are the differences between both magnetic layers in the real and imaginary parts of the optical index, $n=(1-\delta)-i\beta$. Then, to account for the magnetic corrections, each of these layers will have charge and magnetic contributions according to $\delta = \delta_{\text{charge}} \pm \delta_{\text{magnetic}}$, $\beta = \beta_{\text{charge}} \pm \beta_{\text{magnetic}}$, where the sign depends on the sense of the magnetization. Thus, the average values $\bar{\delta}$ and $\bar{\beta}$ include just the charge contributions of each layer and will be the same for both opposite AF states, since both layers have the same thickness. In addition, the product $\Delta\beta\Delta\delta = 4\delta_{\text{magnetic}}\beta_{\text{magnetic}}$ includes just the magnetic contributions and will also be similar and have the same sign for both AF states. So, the application of Eq. (1) to this simple system, including resonant magnetic contributions, indeed predicts a shift $\Delta\theta$ of the AF peak but having the same sense for both AF states, whereas the experimental result shown in Fig. 3(c), corresponding to circular polarization, shows that the shift has opposite signs for both states.

The above discussion suggests that, in addition to refraction/absorption effects, the strong photon polarization dependence of the atomic-scattering factor[28] and the tensor nature of the SXRMS process in multilayers must be considered. This dependence can be observed in Fig. 4, where hysteresis loops have been measured in longitudinal configuration at a fixed location of reciprocal space (around 14°) for the $n=2$ period sample. Two different polarizations have been used, C_+ and linear σ, which is the optimal linear polarization for a longitudinal configuration of the magnetization. Interestingly, both AF states yield a different SXRMS signal intensity $[\delta I(C_+)]$ when it is measured with C_+-polarized photons [Fig. 4(a)], whereas they lead to a similar intensity $[\delta I(\sigma) \approx 0]$ for the measurements with linear-σ polarization [Fig. 4(b)]. This result clearly confirms that circularly polarized photons are able to distinguish the AF state.

One strong advantage of such a simple system, consisting of a $n=2$ period sample, is that an attempt can be made to estimate the expected values of SXRMS signal for both AF states and both polarizations. In order to carry out such a calculation, the starting point is the scattering amplitude, which, including resonant terms in the dipolar approximation,[28] is given by

$$f = -(\boldsymbol{e}_f^* \cdot \boldsymbol{e}_i)[r_e Z - (3\lambda/8\pi)(F_1^1 + F_{-1}^1)] + (3\lambda/8\pi)[-i(\boldsymbol{e}_f^* \times \boldsymbol{e}_i)\cdot \boldsymbol{m}(F_1^1 - F_{-1}^1)], \quad (2)$$

where $\mathbf{e}_\mathbf{i}^*$ and $\mathbf{e}_\mathbf{f}$ give the polarization state of the incident and scattered photons, respectively, r_e is the electron radius, Z is the atomic number, λ is the photon wavelength, and F_i^j are matrix elements containing the energy dependence that includes the resonant behavior. One may define $F^0 = (3\lambda/8\pi)(F_1^1 + F_{-1}^1)$, $F^1 = (3\lambda/8\pi)(F_1^1 - F_{-1}^1)$ as the zero- and first (dipolar)–order resonant factors. The first term of Eq. (2) gives the charge scattering, whereas the sensitivity to the magnetization unitary vector $\mathbf{m}$ is contained in the second term.

Then, the scattered signal for this $n=2$ sample can be modeled as the superposition of two different scattering am-

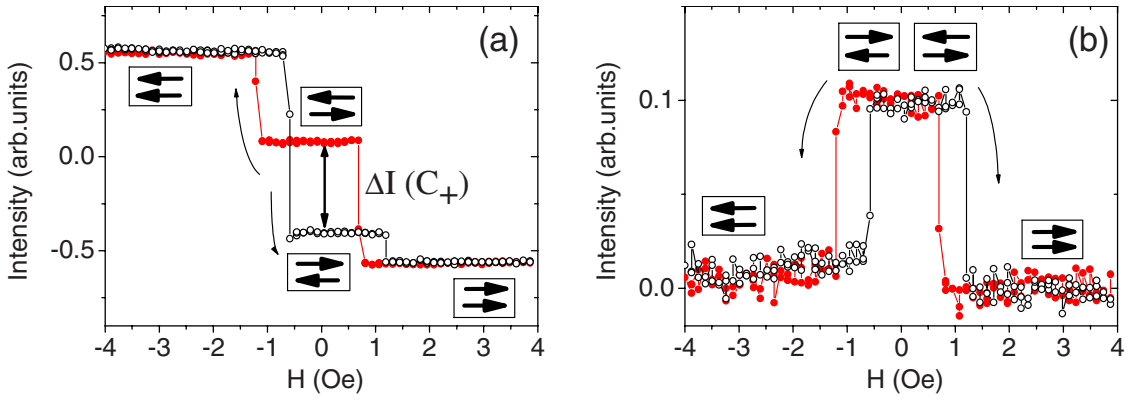

FIG. 4. (Color online) X-ray hysteresis loops of the [Si (30 Å)/$Co_{73}Si_{27}$ (50 Å)]$_2$ multilayer measured in longitudinal configuration with $E=777.6$ eV at $\theta=14°$ with (a) C_+ polarization and (b) linear-σ polarization. Note the different intensity change (ΔI) between the two AF states in each case (loop branches in red and black). The four possible alignments between both magnetic layers are also indicated.

plitudes, one for each magnetic layer, with a relative phase shift, $A(\mathbf{q})=\sigma_{Co}f_A+\sigma_{Co}f_B\exp(-i\mathbf{q}\cdot\mathbf{z}_B)$, where $\mathbf{q}$ is the scattering vector, σ_{Co} is the Co atomic density in the layers, f_j is the resonant scattering amplitude of Co in layer $j=$A, B, and $\mathbf{z}_B$ is the position of layer B (taking the origin at layer B). The strong absorption at a resonant photon energy results in attenuation, which is accounted by considering a complex scattering vector[29] so that $\exp(-i\mathbf{q}\cdot\mathbf{z}_{AB})=\alpha\exp(i\Phi)$ with $\alpha<1$, and then the scattered radiation from layer B presents not only a phase shift relative to layer B but also an amplitude reduction. Combining the expression for $A(\mathbf{q})$ and Eq. (2) and using the matrix formalism of Hill and Mc Morrow[30] leads to:

$$\begin{pmatrix} E_f^s \\ E_f^p \end{pmatrix} \approx \left[\begin{pmatrix} -r_eZ+F^0 & -iF^1 m_{longA}\cos\theta \\ iF^1 m_{longA}\cos\theta & (-r_eZ+F^0)\cos 2\theta \end{pmatrix} + \left[\alpha e^{i\Phi} \begin{pmatrix} -r_eZ+F^0 & -iF^1 m_{longB}\cos\theta \\ iF^1 m_{longB}\cos\theta & (-r_eZ+F^0)\cos 2\theta \end{pmatrix} \right] \times \begin{pmatrix} E_i^s \\ E_i^p \end{pmatrix}, \quad (3)$$

where the incident field can be written as

$$(I_0/2)^{1/2}\begin{pmatrix} 1 \\ i \end{pmatrix}$$

for C_+ photons and

$$(I_0)^{1/2}\begin{pmatrix} 1 \\ 0 \end{pmatrix}$$

for σ photons, and the simplification $m_{polar}=m_{transverse}=0$ has been considered, taking into account the sample well-defined in-plane uniaxial anisotropy (contrary to the usual configuration in other AF systems, where $m_{polar}=m_{longitudinal}=0$ and $m_{transverse}\neq 0$). The resulting intensity difference between both possible AF states is given by

$$\Delta I(C_+) = 2I_0(1+\cos 2\theta)\mathrm{Re}[(-r_eZ+F^0)^*F^1 \times\cos\theta(1-\alpha^2-2i\,\alpha\sin\Phi)], \quad \Delta I(\sigma)=0. \quad (4)$$

This result immediately shows that this qualitative model for the $n=2$ simple case, including absorption/refraction effects, is able to predict a nonvanishing change in intensity at a fixed position in the reciprocal space between the two AF states in the case of C_+ photons and a zero jump for the case of σ photons, in good agreement with the experimental result shown in Fig. 4. This analysis again indicates that absorption/refraction of photons traveling through the layers and charge-magnetic interference, through the $(-r_eZ+F^0)^*F^1$ product, are basic ingredients to understand the observed differences in the SXMRS intensity corresponding to both AF states.

Even more so, Eq. (3) suggests that, as usual in x-ray magnetic circular dichroism measurements, a change from C_+ to C_- polarization should be equivalent to an overall sign change in the magnetization. This symmetry has been indeed observed in the reflectivity curves of the $n=10$ multilayer measured with C_+ and C_- polarization [Fig. 5(a)] that present a similar shift in the half-order AF-peak positions, $\sim 0.5°$, as the one found between the two different remanent AF states in Fig. 3(c). However, it should be noted that in this case, the equivalence is obtained for a condition where the net magnetization of the sample is zero, implying that the C_+/C_- change is equivalent to locally reversing the magnetization in all parts of the sample.

Finally, in order to complete this study, numerical simulations of the reflectivity have been performed using two programs for further reliability, the PPM and REFTOOL codes.[31] These codes have the advantage of including the effects analytically discussed above for simple cases but allowing the computation of more complex situations such as $n=10$ with circular polarization. The x-ray propagation through the multilayer is calculated according to classical electromagnetism, including charge and magnetic resonant contributions to the optical index, that have been derived from C_+ and C_- absorption measurements. The multilayer has been modeled as [Si (31 Å)/$Co_{73}Si_{27}$ (42 Å)]$_{n=10}$, with 3.0 Å total roughness. The experimental reflectivity is shown in Fig. 5(a), with zooms into the 5/2 and 7/2 AF-peak regions in Figs. 5(c) and 5(d), respectively. The calculation [Fig. 5(b) for the whole angular range and Figs. 5(e) and 5(f) for the zooms around the 5/2 and 7/2 AF peaks, respectively]

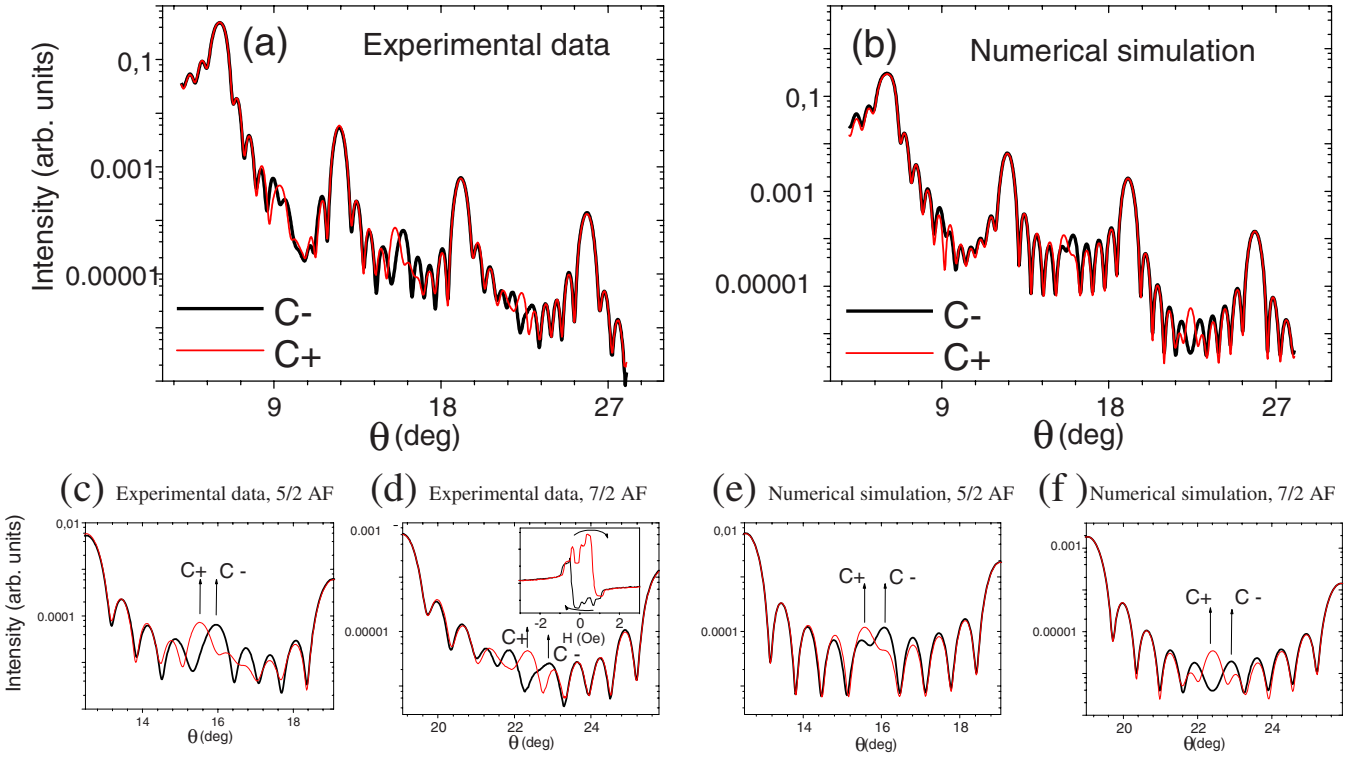

FIG. 5. (Color online) (a) Reflectivities for the $n=10$ multilayer measured at both helicities, C_+ (red thin line) and C_- (black thick line), for remanent state; (b) corresponding numerical simulation using the PPM code; (c) and (d) zooms of the experimental data around the 5/2 AF and 7/2 AF regions, respectively, for C_+ (red) and C_- (black). The inset of (d) shows the hysteresis loop measured at the 7/2 AF peak, at $\theta=22.3°$, for C_+ photons. (e) and (f) show the corresponding numerical simulations of the 5/2 AF and 7/2 AF peaks, respectively, for C_+ (red) and C_- (black).

confirms that the AF peaks' position is sensitive to the photon helicity state or, equivalently, to the AF orientation reversal (not shown but also retrieved). The calculated splitting of about 0.5° for the 5/2 AF peak is in good agreement with the observed one. As a consequence of this sensitivity, the experimental observation of one clear AF peak, higher than the Kiessig fringes and shifting with the polarization, evidences that the illuminated sample area exhibits a clear predominant in-plane AF domain orientation, with alternating magnetization of the layers along the uniaxial easy axis and with no mix of small AF domains with opposite in-plane orientation. In the other case, the incoherent addition of the intensity from similar volumes of two types of opposite domains would lead to a broader and polarization independent AF peak.

It should be pointed out that, although the strongest sensitivity to the photon helicity (or domain orientation) is observed for the 5/2 AF peak, other AF orders, i.e., 3/2 and 7/2, also show marked intensity changes, both in the experiment and simulation (see Fig. 5), confirming the general character of the effect. In relation to this general character, the hysteresis loops measured at AF-peak positions different from the 5/2 one also show the same general behavior, with abrupt jumps and intensity changes dependent on the loop branch [see inset of Fig. 5(d)].

In summary, half-order magnetic peaks have been observed in SXRMS reflectivity curves of $(Si/Co_{73}Si_{27})_{10}$ multilayers taken at remanence, which constitute an unequivocal fingerprint of AF order in these samples. The weak character of the coupling has been clearly established since the AF peaks disappear after applying a magnetic field of about 1 Oe, in good agreement with the information provided by TMOKE measurements. Furthermore, it has been shown that SXRMS is sensitive to the orientation of AF states in magnetic multilayers. That sensitivity was manifested both in the AF-peak hysteresis loops and as an unexpected peak shift of AF order Bragg peaks. The effect has been interpreted as the magnetic analog of anomalous/resonant refraction corrections to the Bragg law and reproduced by numerical simulations.

ACKNOWLEDGMENTS

This work was supported by ESRF and Spanish CICYT (Grants No. FIS2005-07392 and No. NAN2004-09087). Additional funding came from the Spanish Government and the European Social Fund through the "Ramón y Cajal" program (C.Q.), a Spanish MEC "FPU" (L.Z.) grant, and "Organismos Internacionales" and MEC/Fulbright grants (S.M.V.). The authors acknowledge R. Barrett, F. Yakhou, and G. Retout for technical help. S.M.V. thanks J. B. Kortright for helpful scientific discussions and advice.

*Corresponding author. Present address: Materials Science Division, Lawrence Berkeley Laboratory, Berkeley, CA 94720, USA. smvalvidaressuarez@lbl.gov

†Present address: Synchrotron SOLEIL/L'Orme des Merisiers, Saint-Aubin, BP 48, 91192 Gif-sur-Yvette, France.

‡Present address: Diamond Light Source Ltd, Didcot, OX11 0DE, United Kingdom.

[1] Sean Langridge, Jörg Schmalian, C. H. Marrows, D. T. Dekadjevi, and B. J. Hickey, Phys. Rev. Lett. **85**, 4964 (2000).

[2] M. R. Fitzsimmons, S. D. Bader, J. A. Borchers, G. P. Felcher, J. K. Furdyna, A. Hoffmann, J. B. Kortright, I. K. Schuller, T. C. Schulthess, S. K. Sinha, M. F. Toney, D. Weller, and S. Wolf, J. Magn. Magn. Mater. **271**, 103 (2004).

[3] Doon Gibbs, D. R. Harshman, E. D. Isaacs, D. B. McWhan, D. Mills, and C. Vettier, Phys. Rev. Lett. **61**, 1241 (1988).

[4] J. M. Tonnerre, L. Sève, D. Raoux, G. Soullié, B. Rodmacq, and P. Wolfers, Phys. Rev. Lett. **75**, 740 (1995).

[5] M. Hecker, S. Valencia, P. M. Oppeneer, H.-Ch. Mertins, and C. M. Schneider, Phys. Rev. B **72**, 054437 (2005).

[6] J. B. Kortright, D. D. Awschalom, J. Stöhr, S. D. Bader, Y. U. Idzerda, S. S. P. Parkin, Ivan K. Schuller, and H.-C. Siegmann, J. Magn. Magn. Mater. **207**, 7 (1999), and references therein.

[7] T. P. A. Hase, I. Pape, B. K. Tanner, H. Dürr, E. Dudzik, G. van der Laan, C. H. Marrows, and B. J. Hickey, Phys. Rev. B **61**, R3792 (2000).

[8] C. Spezzani, P. Torelli, M. Sacchi, R. Delaunay, C. F. Hague, F. Salmassi, and E. M. Gullikson, Phys. Rev. B **66**, 052408 (2002).

[9] C. H. Marrows, P. Steadman, A. C. Hampson, L.-A. Michez, B. J. Hickey, N. D. Telling, D. A. Arena, J. Dvorak, and S. Langridge, Phys. Rev. B **72**, 024421 (2005).

[10] Y. U. Idzerda, V. Chakarian, and J. W. Freeland, Phys. Rev. Lett. **82**, 1562 (1999).

[11] Maurizio Sacchi, Coryn F. Hague, Luca Pasquali, Alessandro Mirone, Jean-Michel Mariot, Peter Isberg, Eric M. Gullikson, and James H. Underwood, Phys. Rev. Lett. **81**, 1521 (1998).

[12] M. Blume, J. Appl. Phys. **57**, 3615 (1985); S. Ferrer, P. Fajardo, F. de Bergevin, J. Alvarez, X. Torrelles, H. A. van der Vegt, and V. H. Etgens, Phys. Rev. Lett. **77**, 747 (1996); E. E. Fullerton, O. Hellwig, K. Takano, and J. B. Kortright, Nucl. Instrum. Methods Phys. Res. B **200**, 202 (2003); Sang-Koog Kim and J. B. Kortright, Phys. Rev. Lett. **86**, 1347 (2001).

[13] C. Spezzani, P. Torelli, M. Sacchi, R. Delaunay, C. F. Haque, V. Cros, and F. Petroff, Appl. Phys. Lett. **81**, 3425 (2002); J. W. Freeland, K. Bussmann, Y. U. Idzerda, and C.-C. Kao, Phys. Rev. B **60**, R9923 (1999); J. F. MacKay, C. Teichert, D. E. Savage, and M. G. Lagally, Phys. Rev. Lett. **77**, 3925 (1996); M. Sacchi, C. F. Hague, L. Pasquali, A. Mirone, J. M. Mariot, P. Isberg, E. M. Gullikson, and J. H. Underwood, *ibid.* **81**, 1521 (1998); S. S. Roy, M. R. Fitzsimmons, S. Park, M. Dorn, O. Petracic, Igor V. Roshchin, Zhi-Pan Li, X. Batlle, R. Morales, A. Misra, X. Zhang, K. Chesnel, J. B. Kortright, S. K. Sinha, and Ivan K. Schuller, *ibid.* **95**, 047201 (2005).

[14] D. R. Lee, S. K. Sinha, D. Haskel, Y. Choi, J. C. Lang, S. A. Stepanov, and G. Srajer, Phys. Rev. B **68**, 224409 (2003); D. R. Lee, S. K. Sinha, C. S. Nelson, J. C. Lang, C. T. Venkataraman, G. Srajer, and R. M. Osgood, *ibid.* **68**, 224410 (2003).

[15] H. A. Dürr, E. Dudzik, S. S. Dhesi, J. B. Goedkoop, G. van der Laan, M. Belakhovsky, C. Mocuta, A. Marty, and Y. Samson, Science **284**, 2166 (1999).

[16] J. B. Kortright, Sang-Koog Kim, G. P. Denbeaux, G. Zeltzer, K. Takano, and Eric E. Fullerton, Phys. Rev. B **64**, 092401 (2001); O. Hellwig, J. B. Kortright, K. Takano, and Eric E. Fullerton, *ibid.* **62**, 11694 (2000).

[17] B. Briner and M. Landolt, Phys. Rev. Lett. **73**, 340 (1994).

[18] K. Inomata, K. Yusu, and Y. Saito, Phys. Rev. Lett. **74**, 1863 (1995).

[19] E. E. Fullerton and S. D. Bader, Phys. Rev. B **53**, 5112 (1996).

[20] R. R. Gareev, D. E. Bürgler, M. Buchmeier, D. Olligs, R. Schreiber, and P. Grünberg, Phys. Rev. Lett. **87**, 157202 (2001).

[21] P. J. Grundy, J. M. Fallon, and H. J. Blythe, Phys. Rev. B **62**, 9566 (2000).

[22] C. Quirós, J. I. Martín, L. Zárate, M. Vélez, and J. M. Alameda, Phys. Rev. B **71**, 024423 (2005).

[23] L. Zárate, C. Quirós, M. Vélez, G. Rodríguez-Rodríguez, J. I. Martín, and J. M. Alameda, Phys. Rev. B **74**, 014414 (2006).

[24] N. Yaacoub, C. Meny, O. Bengone, and P. Panissod, Phys. Rev. Lett. **97**, 257206 (2006).

[25] R. W. James, *The Optical Principles of the Diffraction of X-Rays* (Cornell University, Ithaca, NY, 1965).

[26] Alan E. Rosenbluth and P. Lee, Appl. Phys. Lett. **40**, 466 (1982).

[27] J. B. Kortright and S.-K. Kim, Phys. Rev. B **62**, 12216 (2000).

[28] J. P. Hannon, G. T. Trammell, M. Blume, and Doon Gibbs, Phys. Rev. Lett. **61**, 1245 (1988).

[29] L. Seve, J. M. Tonnerre, and D. Raoux, J. Appl. Crystallogr. **31**, 700 (1998).

[30] J. P. Hill and D. F. McMorrow, Acta Crystallogr., Sect. A: Found. Crystallogr. **52**, 236 (1996).

[31] PPM code developed by A. Mirone (mirone@esrf.fr); REFTOOL code developed by E. Bontempi, N. Jaouen, and J. M. Tonnerre (jeanmarc.tonnerre@grenoble.cnrs.fr).